Study on the Phase Behavior of Ethylene–Vinyl Acetate Copolymer and Poly(methyl methacrylate) Blends by *In Situ* Polymerization

Shih-Kai Cheng, Chuh-Yung Chen

Department of Chemical Engineering, National Cheng-Kung University, Tainan, Taiwan 70101

Received 24 October 2002; accepted 16 January 2003

ABSTRACT: This study examines the phase behavior of ethylene–vinyl acetate copolymer (EVA) and poly(methyl methacrylate) (PMMA) blends during MMA polymerization. The ternary PMMA/MMA/EVA mixtures are considered to create a triangular phase diagram, which responds the phase changes during polymerization. The phase changes during MMA polymerization are also examined by optical microscope and photometer. Since the PMMA and EVA are well-known immiscibles, the polymer solution undergoes phase separation at the initial stage of the MMA polymerization. Additionally, the phase inversion occurs as the conversion of MMA between 13.8 and 20.8%. On the other hand, the EVA-graft-PMMA, which can reduce the dispersed EVA particle size, is induced efficiently by taking *tert*-butyl peroctoate (*t*-BO) as initiator during MMA polymerization. © 2003 Wiley Periodicals, Inc. J Appl Polym Sci 90: 1001–1008, 2003

Key words: blends; graft copolymers; phase behavior; phase diagrams; phase separation

INTRODUCTION

In most cases, melt mixing two polymers results in blends that are weak and brittle; while the low deformation modulus may follow an approximately linear mixing rule, the ultimate properties certainly will not. This is because the incorporation of a dispersed phase in a matrix leads to the presence of stress concentrations and weak interfaces, arising from poor mechanical coupling between phases. It is most common for compatibilization to be achieved by addition of a third component, or by *in situ* chemical reaction, leading to modification of the polymer interfaces in two-phase blends, and thereby to tailoring of the phase structure, and hence properties.[1] The mechanical properties of a blend or alloy will be determined not only by the properties of its components, but also by the phase morphology and the interphase adhesion, both of which are important from the viewpoint of stress transfer within the blend in its end-use application. The phase morphology will be normally determined by the processing history to which the blend has been subjected.

The common commercialized blend product is high-impact polystyrene (HIPS). In the research of HIPS, dispersed rubber particles with subinclusions of polystyrene (PS), constituting the so-called salami structure, are crucial in rubber-toughened PS. In the PS/styrene (SM)/polybutadiene (PB) polymerization system,[2,3] phase separation results in immediate formation of droplets of a PS/SM phase in a continuous PB/SM phase in the initial polymerization period. The PS and PB chains with the PS graft copolymer participate in the beginning of phase separation and form an interface between PS and PB phases.[4–6] With further polymerization, the volume of the PS/SM phase increases until the volume of PS/SM and PB/SM are equal. At this stage, the dispersed PS/SM phase becomes the continuous phase and the PB/SM phase becomes the dispersed droplets—in other words, phase inversion occurs. Furthermore, the unreacted SM in the dispersed and continuous phases proceeds to complete the polymerization; thus the dispersed PB phase traps some PS to form a salami structure.[7,8] This structure causes the volume fraction of the dispersed phase to exceed the volume fraction of the added rubber, which can improve the toughness of the PS matrix.

Ethylene–vinyl acetate (EVA) elastomer is a suitable material to toughen PMMA because the whole chemical chain of EVA is saturated and elastic. Besides, the refractive index of EVA is very close to the PMMA and hence the transparent PMMA blends can be possibly produced. In studies using EVA as the toughening agent, the mechanical blend caused larger rubber particles, resulting in poorer toughness.[9–11] In the previous work,[12] the transparent toughened poly(methyl

Correspondence to: C.-Y. Chen (ccy7@ccmail.ncku.edu.tw).
Contract grant sponsor: National Science Council of the Republic of China; contract grant number: NSC 91-2216-E-006-022.

TABLE I
The Recipe of Light Transmittance-Composition Measurements

MMA (%)	EVA (%)/PMMA (%)[a]					
96	0.2/3.8	0.6/3.4	1.0/3.0	3.0/1.0	3.4/0.6	3.8/0.2
94	0.3/5.7	0.9/5.1	1.5/4.5	4.5/1.5	5.1/0.9	5.7/0.3
92	0.4/7.6	1.2/6.8	2.0/6.0	6.0/2.0	6.8/1.2	7.6/0.4

[a] EVA(%) + PMMA(%) = 100-MMA(%). The ratios of EVA(%)/PMMA(%) from left to right are 5/95, 15/85, 25/75, 75/25, 85/15, and 95/5, respectively.

methacrylate) (PMMA) sheets are available by introducing the EVA into *in situ* polymerization of MMA. Therefore, the phase behaviors of PMMA/MMA/EVA mixtures during the polymerization should be involved. This study constructs the triangular phase diagram of the ternary PMMA/MMA/EVA system. Combining the observation from the optical microscope (OM) at various reaction times during the MMA polymerization with the triangular phase diagram, the phase behaviors can be clearly illustrated. The final morphologies of blends, which are produced by peroxide and azo initiator, are also discussed.

EXPERIMENTAL

Preparation of PMMA/MMA/EVA triangular phase diagram

The phase diagram of the PMMA/MMA/EVA ternary solution was measured by the visible absorption spectroscopy method: a transparent mixture in a reactor with a condensation system at 100°C was cooled down to various temperatures (from 95 to 60°C, the decrement was 5°C) and the light transmittance was measured by the visible absorption spectroscopy at λ = 546 nm at each temperature. The PMMA used in this experiment was a commercialized product (ACRYREX® CM-205, kindly supplied by Chi-Mei Corporation, Tainan, Taiwan, China), and its M_w and M_w/M_n measured by GPC were 79400 and 1.73, respectively. EVA with 18 wt % VA content and 0.75 melt index flow and commercial grade MMA, which was purified by distillation, were used in the experiment. An inhibitor, 1,4-benzoquinone (0.1 wt %), was added to the ternary solution to prevent thermal polymerization of MMA during spectroscopy measurement. The recipes are listed in Table I.

Phase change during polymerization

Thirty grams of EVA was dissolved in 270 g MMA to produce the bulk polymerization at 90°C, using a constantly rotating stirrer. Polymerization proceeded after adding 0.3g *tert*-butyl peroctoate (*t*-BO). Some solution was extracted and weighted, and some solution was coated onto a slide and covered with another slide every 5 min. Each extracted solution was precipitated by methanol and filtered, then vacuum dried and weighted. The conversion vs time curve was thus obtained. The coated solutions at various times were used to study the phase change during polymerization by OM. A photometer was employed to detect the intensity of the transmitted light while the phase behavior was observed by OM. In order to avoid the unnecessary effect of temperature changes, a thermocontroller was applied to maintain the observation temperature at 90°C.

The preparation of EVA/PMMA sheets

MMA was added to the Pyrex reactor and mixed with EVA at 90°C. While EVA dissolved, polymerization proceeded after the addition of *t*-BO, according to the specification of Table II. After polymerization reached a high limit of viscosity, 700 g of MMA monomer preheated at 60°C was poured into the reactor; meanwhile, the reaction temperature was lowered to 40°C. Thus the solution is less viscous and suitable for the casting process. EVA/PMMA sheets of 3 mm thick were prepared by pouring the solution into a cell comprising two tempered glass plates with a polyvinylchloride (PVC) spacer and then closed. The polymerization was carried out quiescently in a water bath kept at 60°C for 4 h. To complete the reaction, the sheets were further annealed at 100°C in an oven for 1 h.

Grafting level

In order to calculate the grafting level in the EVA/PMMA sheet, the homopolymer of PMMA should be removed. Since the PMMA is easily dissolved in acetone, some casting products were extracted by acetone at 50°C. Then the solution was separated by a centrifuge at 10000 rpm for 30 min after the solution cooled. Two distinguishable layers were observed. The upper solution was dried and the lower precipitate was extracted by acetone again. Until the upper solution

TABLE II
The Recipe of EVA Toughened PMMA Sheet

Sample[a]	EVA (wt %)	EVA (g)	MMA (g)[b] 1st	MMA (g)[b] 2nd	AIBN (g)	*t*-BO (g)
MIL3	3	30	270	700	0	0.6
MIL6A	6	60	240	700	0.6	0
MIL6	6	60	240	700	0	0.6
MIL10	10	100	200	700	0	0.6

[a] MIL: VA content = 18 wt %, MI = 0.7.
[b] 1st: To dissolve EVA before initiator added.
2nd: Added for a suitable viscosity of casting process.

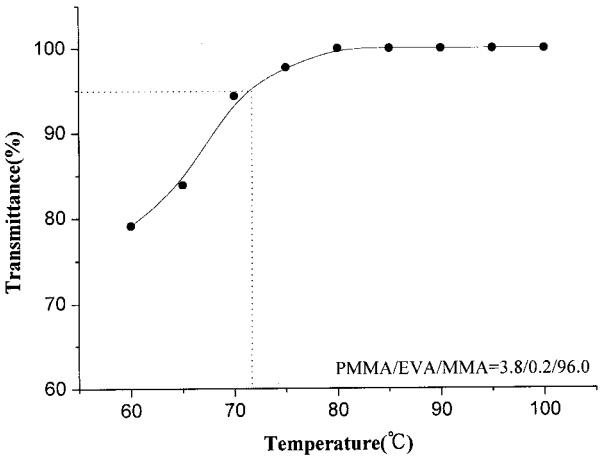

Figure 1 The light transmittance vs temperature at a certain composition.

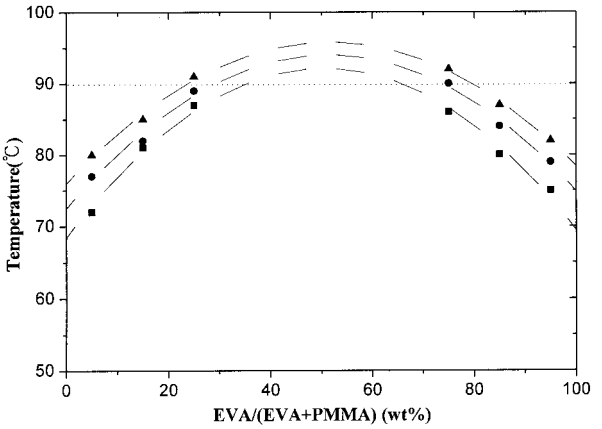

Figure 2 Temperature vs EVA/PMMA compositions at various MMA wt %: (■) 96, (●) 94, and (▲) 92.

contained nothing after drying, the precipitate was dried in a vacuum oven, weighted, and examined by differential scanning calorimetry (DSC, TA DSC2910, scan rate is 10°C /min). The grafting level was calculated as follows:

$$\text{Grafting level} = \frac{\text{amount of dry precipitate} - \text{amount of EVA}}{\text{amount of EVA}} \times 100\% \quad (1)$$

Morphology identification

A transmission electron microscope (TEM, Joel 2010) was used to observe ultramicrotome sections of the EVA/PMMA sheets (MIL6 and MIL6A), which was stained by 1% osmium tetroxide vapors at room temperature for 2 h.

RESULTS AND DISCUSSION

PMMA/EVA/MMA phase behaviors

Phase diagram

Figure 1 shows the light transmittance vs temperature at a certain composition (PMMA/EVA/MMA=3.8/0.2/96.0). The curve shows that the light transmittance is nearly constant above 80°C, and then decreases with the temperature. During the cooling procedure after 80°C, some dispersed cotton-like materials, which can be observed by the naked eye, exist in the solution. The incident light is scattered by the dispersed materials, which results in the decreased light transmittance. When the temperature is cooled down from 65 to 60°C, a cloudy solution can be observed. At that moment, the light transmittance is already lowered to 80%. In this article, we assign 5% light transmittance loss as the phase separation point. After combining the phase separation points of all compositions in Table I, the phase separation curves of the ternary PMMA/EVA/MMA mixtures can be plotted, as shown in Figure 2. Upper critical solution temperature (UCST) type phase behavior can be obtained. From these phase separation curves, one can draw a triangular phase diagram at a fixed temperature. Since the reaction proceeds at 90°C, the dotted line in Figure 2 has two crossed points with each phase separation curve. The phase separation compositions of PMMA/EVA/MMA at 90°C are determined. The triangular phase diagram at 90°C can be plotted, as shown in Figure 3. As represent in the diagram, there is a small single-phase region in the top of the diagram. Most of the ternary PMMA/EVA/MMA systems are in the two-phase region.

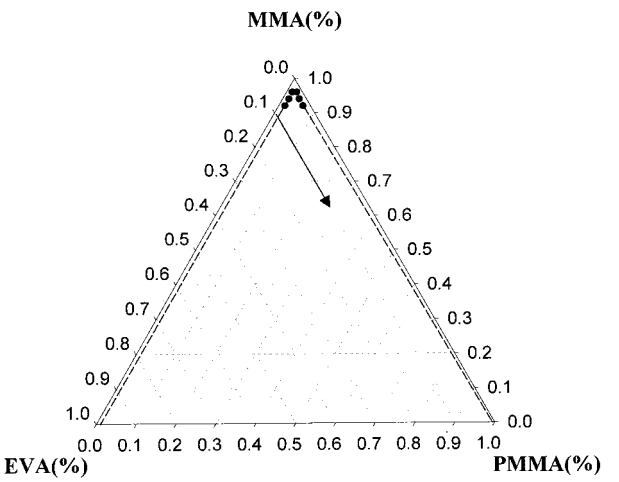

Figure 3 The triangular phase diagram of the ternary PMMA/EVA/MMA system at 90°C.

Thermodynamics of PMMA/EVA/MMA ternary systems

In the view of thermodynamics, the modification of the classical Gibbs' free energy change of mixing (ΔG_m)[13] can be represented as follows:

$$\frac{\Delta G_m}{kT} = \underbrace{N_1 \ln \nu_1 + \frac{N\nu_2}{x_2} \ln \nu_2 + \frac{N\nu_3}{x_3} \ln \nu_3}_{\text{Entropy term}} + \underbrace{(N_1 + x_2N_2 + x_3N_3)\,(\chi_{12}\nu_1\nu_2 + \chi_{13}\nu_1\nu_3 + \chi_{23}\nu_3\nu_3)}_{\text{Enthalpy term}}$$

where

$$\nu_1 = \frac{N_1}{N},\ \nu_2 = \frac{x_2N_2}{N},\ \nu_3 = \frac{x_3N_3}{N},\ N = N_1 + x_2N_2 + x_3N_3$$

1 indicates the monomer, 2,3 indicate the polymer, x_I indicates segments of each molecular chain of the ith component, N_I indicates the total numbers of the ith component, ν_i indicates the volume fraction of the ith component, and χ_{ij} indicates the interaction parameter between components i and j.

The first three terms can be concluded as the contribution of the entropy and the last one is related to the enthalpy contribution. In the entropy term, since the volume fraction, ν_1, ν_2, and ν_3 are all less then 1, the entropy change of mixing (ΔS_m) is negative and the absolute value of ΔS_m decreases with increasing the conversion of PMMA. In the enthalpy term, the enthalpy value depends on the solution parameters (χ_{ij}). For many nonpolar polymer–solvent systems, solution parameters are positive. Hence, the χ_{12} and χ_{13} are positive. The χ_{23} represents the exchange of local free energy (Δw) when the EVA segment is mixed with the PMMA segment. When x_2 and x_3 are sufficiently large, χ_{23} at the critical point of this mixture approaches zero. According to Kurata,[13] if the London dispersion forces dominate molecular interactions, the energy of creating molecular contacts between different species is positive. This indicates that $\Delta w \geqq 0$, because each molecule may be placed by a segment of a particular polymer chain. The value of χ_{23} for EVA and PMMA is positive. Thus, the enthalpy change of mixing (ΔH_m) is positive and the value of ΔH_m increases with the conversion of PMMA. After the combination of entropy and enthalpy terms, a positive ΔG_m is found. Therefore, the PMMA/EVA/MMA ternary system becomes thermodynamically immiscible as polymerization proceeds to a certain conversion.

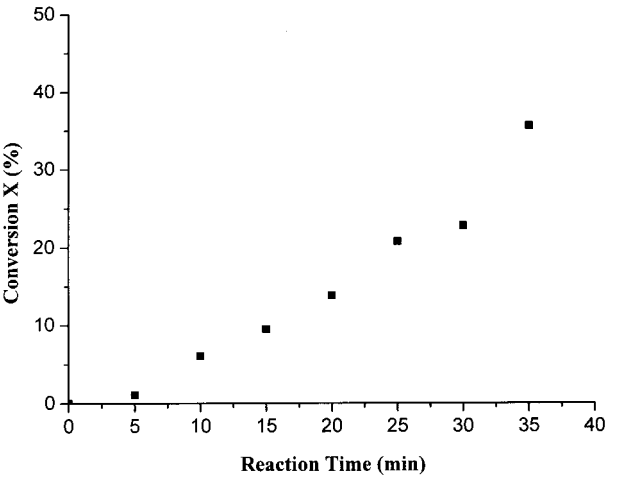

Figure 4 The curve of MMA conversion vs time.

Phase behaviors during polymerization

With the phase diagram, the morphology of phase behavior of PMMA/EVA/MMA during the MMA polymerization is concerned. In the most incompatible reactive polymer blends (e.g., HIPS), there exists a phase inversion behavior at a certain conversion of monomer. In the experiment of phase change during polymerization, the EVA content is fixed at 10 wt % and the polymerization is initiated by t-BO at 90°C, as described in the section Phase Change During Polymerization above. The arrow in Figure 3 indicates the direction of the polymerization. By sampling the mixture every 5 min during polymerization, the time-conversion curve at 90°C can be observed, as displayed in Figure 4. Combining Figure 3 and Figure 4, one can observe that the system transfers from the one-phase to the two-phase regime when the polymerization proceeds at very low MMA conversion.

Figures 5 and 6 record the optical microscopy pictures of phase behavior during polymerization for a conversion up to 35.6% and the relation of the light transmittance to MMA conversion, respectively. Since 10 wt % EVA can completely dissolve in MMA at 90°C, the solution is homogeneous at the initial stage of polymerization and the light transmittance is 100%, as shown in Figure 5(a) and Figure 6. Figure 5(b) shows that phase separation occurs when conversion reaches 1.1%, because of the formation of second phase. However, PMMA is not miscible in EVA/MMA domain because $\Delta G_m > 0$, as described before. The PMMA/MMA should become a dispersed phase in the EVA/MMA continuous phase. Figure 6 shows that the light transmittance has an obviously change between 0 and 9.5% conversion, which is caused by the light scattering of the separated droplets. This result is consistent with the triangular phase diagram, which also shows that when conversion is between 0 and 6.0% the ternary system already transfers from the

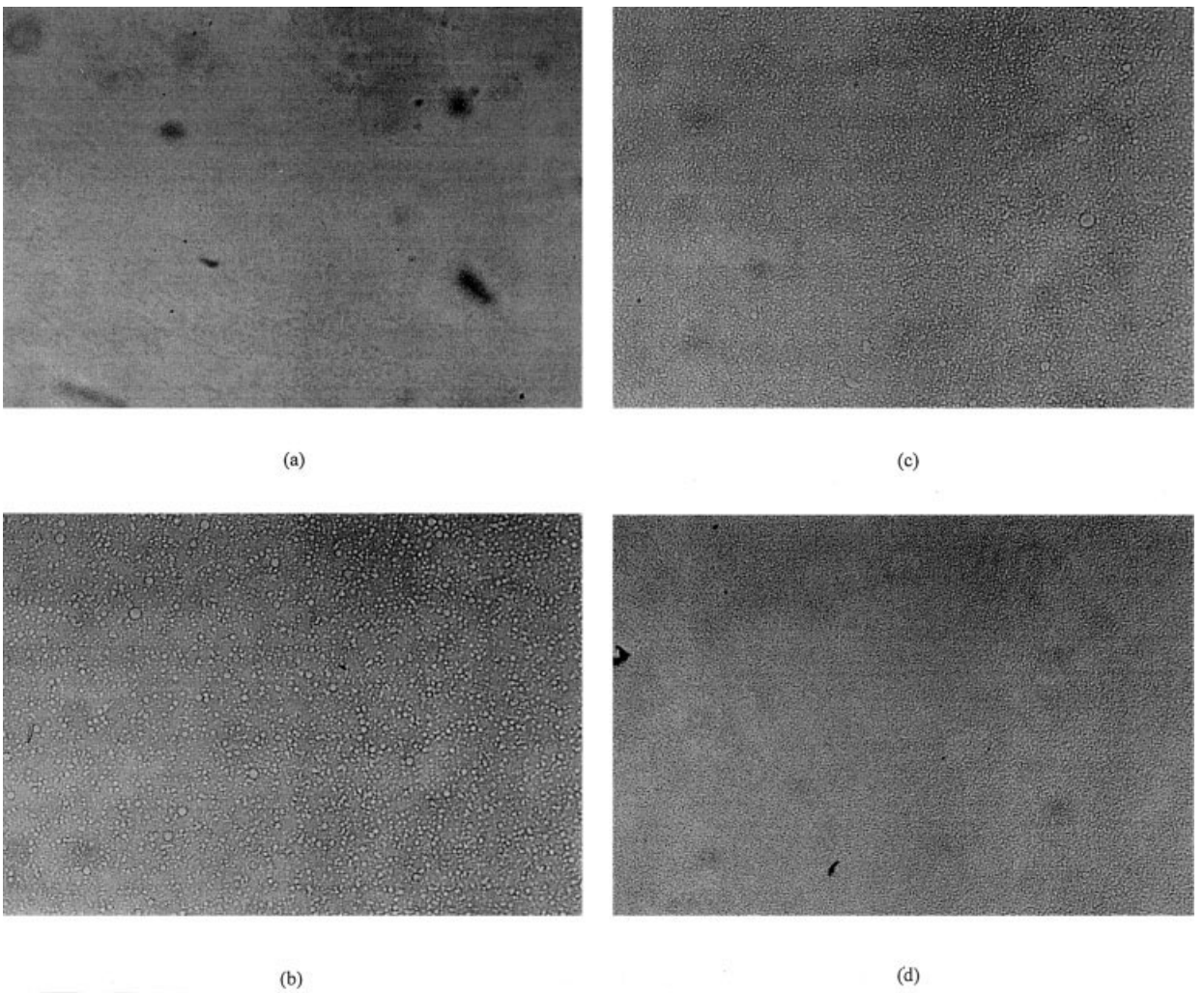

Figure 5 Pictures of phase observation by OM at various reaction times/conversions: (a) 0 min/0 (200×), (b) 5 min/1.1 (200×), (c) 10 min/6.0 (200×), (d) 15 min/9.5 (200×), (e) 20 min/13.8 (200×), and (f) 25 min/20.8 (200×).

one-phase to two-phase region. After phase separation, more and more incident lights are scattered or refracted by the generated boundary of the dispersed phase [Fig. 5(c) and 5(d)]. As the conversion reaches 13.8%, the light transmittance locates at the minimum of the curve in Figure 6. At this moment, in comparison with Figure 7, the phase volume ratio of EVA/PMMA is approximately unity (X=13.8%). In Figure 5(e) and 5(f), the morphology of the interconnected worm-like structure can be observed in the picture. The worm-like structure is a symbol, indicating that the system is undergoing spinodal decomposition.[14] From conversion 13.8 to 20.8%, the light transmittance raise to a local maximum, there should exist the continuous phase change at this stage. In the ternary PMMA/EVA/MMA system, the continuous phase must change from EVA/MMA to PMMA/EVA. Hence, the phase inversion takes place. After phase inversion, the light transmittance decreases again. Finally, the opaque solution is formed and the light transmittance is below 80% at the conversion 35.6%. In conclusion, the results of OM pictures and the light transmittance show that the ternary system undergoes phase separation in the initial stage of the polymerization (1.1% conversion) and exhibits a phase inversion that accompanies the spinodal decomposition when the MMA conversion is between 13.8 and 20.8%.

Effect of grafted PMMA

Homopolymer PMMA in the EVA/PMMA sheet can be extracted by acetone at 50°C. After the centrifugation, the solution is separated into two parts, the lower precipitate and the upper solution. Since EVA does not dissolve in acetone at room temperature, the precipitate is the mixture of EVA-g-PMMA/EVA. The clear and viscous solution consists of PMMA/acetone. Both precipitate and solution are dried in vacuum oven at room temperature for three days. The grafting level of precipitate is determined by eq. (1) and listed in Table III. DSC is utilized to analyze the dried precipitates. A comparison with the pure EVA in Table III

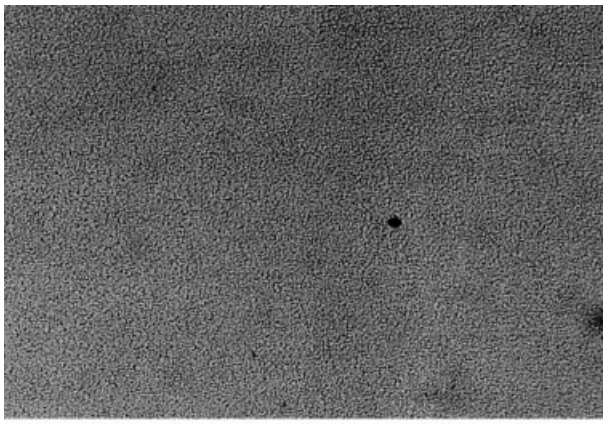

(c)

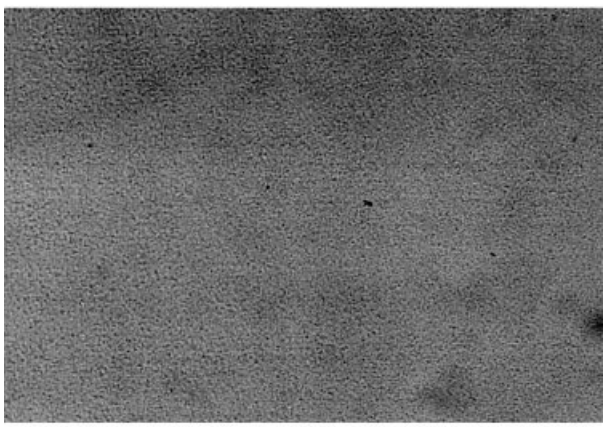

(f)

Figure 5 (*Continued from previous page*)

shows that T_m and T_c of the EVA-g-PMMA decreases with grafting level. Besides, an obvious glass transition temperature of the grafted PMMA can be obtained in grafted copolymers. The glass transition signal is apparent while the graft level is larger than 250%. It is well known that the crystallinity of the EVA copolymer is provided by the polyethylene sequences of the backbone. In order to exclude the vinyl acetate (VA) segments during crystallization, smaller and imperfect spherulites are formed. The magnitude of destroyed crystallinity is increased with the amount of VA content. Thus, the crystallinity is also destroyed by the grafted PMMA. The decreased T_m and T_c illustrate the influence of grafted PMMA chain. From grafting level and DSC results, the heat of fusion (ΔH_f) and the heat of crystallization (ΔH_c) of EVA-g-PMMA can be compared with those of pure EVA and can determine

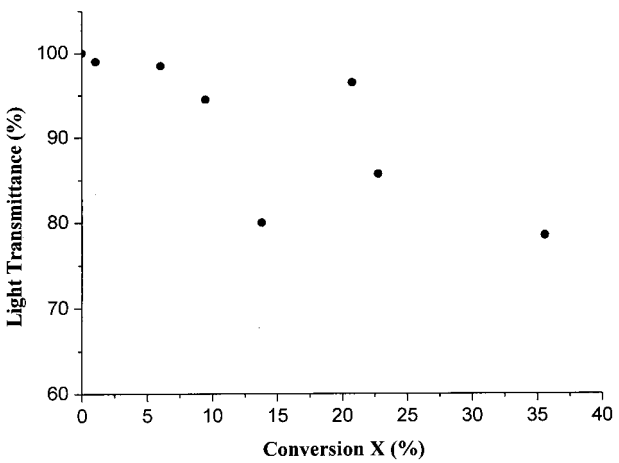

Figure 6 The curve of percentage light transmittance observed by photometer vs MMA conversion.

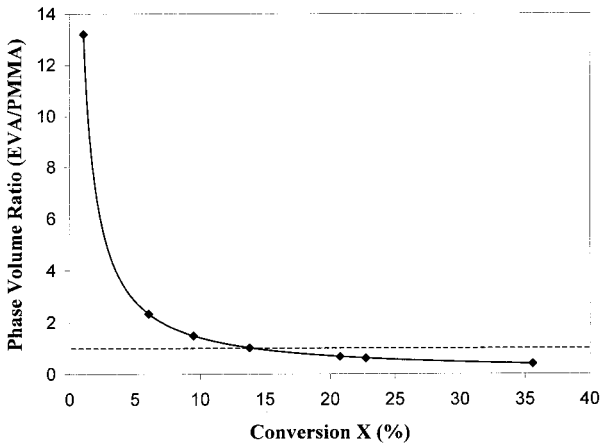

Figure 7 Phase volume ratio of EVA/PMMA vs MMA conversion.

TABLE III
Summary of Grafting Level and DSC Results

		EVA-graft-PMMA			
	EVA	MIL3	MIL6A	MIL6	MIL10
Grafting level (%)		322	43	250	175
T_g (°C)		115.5	—	106.2	—
T_m (°C)	86.9	80.8	85.5	82.5	83.6
ΔT_m (°C)		−6.1	−1.4	−4.4	−3.3
T_c (°C)	67.7	59.0	66.1	60.4	64.5
ΔT_c (°C)		−8.7	−1.6	−7.3	−3.2
ΔH_f (J/g)					
Exp.	50.96	6.70	19.73	10.30	14.37
Theor.[a]		12.07	21.75	14.57	18.53
ΔH_c (J/g)					
Exp.	55.78	7.54	21.31	11.96	15.95
Theor.		13.21	23.81	19.94	20.28
Relative X_c[b] (%)		55.5	90.7	70.7	77.5

[a] ΔH(Theor.) calculated from ΔH of pure EVA, taking into account the weight percentage of EVA in the EVA-g-PMMA.

[b] X_c = percent crystallinity related to EVA content in the EVA-g-PMMA. $X_c = [\Delta H_f(\text{Exp.})/\Delta H_f(\text{Theor.})] \times 100\%$.

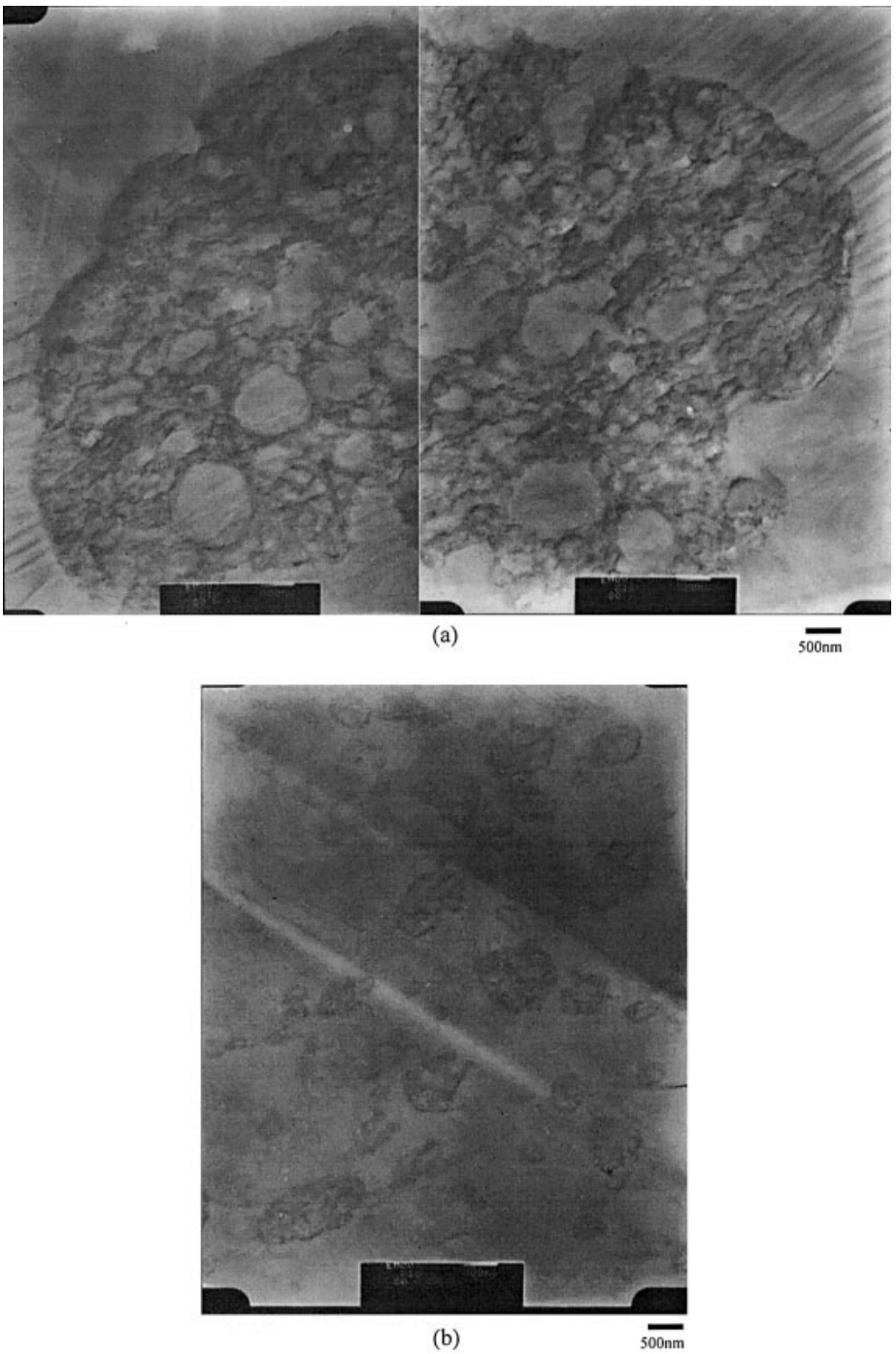

Figure 8 The TEM photos of (a) MIL6A and (b) MIL6.

the relative crystallinity (X_c) of EVA-g-PMMA. The more PMMA graft onto the EVA, the less crystallinity is formed.

There is evidence indicating that the peroxide radicals are more efficient for inducing the graft copolymerization than the azo radicals.[15–20] Thus, the grafting level of MIL6, which is initiated by *t*-BO, is much higher than initiated by AIBN (MIL6A) in Table III. The DSC results show that T_m and T_c of MIL6A are not obviously decreased. The PMMA homopolymer and the PMMA grafted to the EVA copolymer can be induced efficiently during MMA polymerization by taking *t*-BO as initiator. From the TEM photograph of MIL6A (Fig. 8), there are many more subinclusions than MIL6 enclosed within the EVA domain. TEM photos also show how the graft copolymer affects the particle size. The graft copolymer acts as compatibilizer, which can reduce the interfacial tension in the blends, cause an emulsifying effect, and lead to an extremely fine dispersion of EVA phase in PMMA

phase. Therefore, different from MIL6A, a smaller particle size about 1 μm can be found in the TEM photo of MIL6.

CONCLUSION

According to the phase diagram and the pictures observed by OM, the ternary MMA/EVA/PMMA system is first formed as a homogeneous solution before polymerization. After addition of initiator, the system is then quickly phase separated at very low MMA conversion (1.1% conversion). When the conversion reaches 13.8%, the phase inversion starts. Until conversion reaches 20.8%, the continuous phase has been fully inverted from EVA/MMA to PMMA/MMA. Since the ethylene backbone of EVA is a good chain transfer active site, PMMA grafting EVA copolymerization will occur during MMA polymerization. After observation by TEM, the graft copolymer, which is induced by the peroxide radical, results in the fine dispersed EVA particles in the PMMA matrix.

References

1. Bonner, J. G.; Hope, P. S. Polymer Blends and Alloys; Chapman & Hall: Glasgow, 1993; Chap 3.
2. Kruse, R. L. Adv Chem Ser 1969, 142, 141.
3. White, J. L.; Patel, R. D. J Appl Polym Sci 19 1975, 1775.
4. Molau, G. E.; Keskkula, H. J Polym Sci, Part A-1 1966, 4, 1595.
5. Kohler, J.; Riess, G.; Banderet, A. Angew Makromol Chem 1971, 15, 55.
6. Patel, P. G.; Craig, T. O. J Polym Sci, Part A-1 1972, 10, 1867.
7. Bwnder, B. W. J Appl Polym Sci 1965, 9, 2887.
8. Qiyun, Z.; Renyun, P.; Shengying, T.; Huigen, Y. Chem Eng Chin Univ 1993, 7(4), 394.
9. Deanin, R. D.; Pickett, T. J.; Huang, J. C. Polym Mater Sci Eng 1989, 61, 950.
10. Soares, B. G.; Barbosa, R. V.; Covas, J. C. J Appl Polym Sci 1997, 65, 2141.
11. Barbosa, R. V.; Moraes, M. A. R.; Gomes, A. S.; Soares, B. G. Macromol Rep 1995, A32(5&6), 663.
12. Cheng, S. K.; Chen, C. Y. Eur Polym J, 2002, submitted.
13. Kurata, M. Thermodynamics of Polymer Solutions, Vol. 1; Hardwood Academic Publishers: New York, 1982.
14. Reich, S. Phy Lett 1986, 114A(2), 90.
15. Brydon, A.; Burnett, G. M.; Gameron, G. G. J Polym Sci, Polym Chem Ed 1973, 11, 3255.
16. Brydon, A.; Burnett, G. M.; Gameron, G. G. J Polym Sci, Polym Chem Ed 1974, 12, 1011.
17. Gameron, G. G.; Quereshi, M. Y. J Polym Sci, Polym Chem Ed 1980,18, 2143.
18. Gameron, G. G.; Quereshi, M. Y. J Polym Sci, Polym Chem Ed 1980, 18, 3149.
19. Madhah, A. G.; Amin, M. B.; Usmani, A. M. Polym Bull 1985, 14, 433.
20. Alberts, H.; Bartl, H.; Kuhn, E. Adv Chem Ser 1975, 142, 214.